# Systematic Mathematical Strategies for Superparameterization with Moderate Scale Gaps and No Invariant Measure: Application to Squall Lines

*By Andrew J. Majda*
*Morse Professor of Arts and Sciences*
*Department of Mathematics*
*And*
*Center for Atmospheric Ocean Sciences*
*Courant Institute of Mathematical Sciences, NYU*

Lecture is based on four recent papers:

1. A. Majda and M. Grote, "Mathematical Test Models for Superparameterization in Anisotropic Turbulence," PNAS, April 2009, Vol. 106, no. 14, pp. 5470 – 5476
2. A. Majda and Y. Xing, "New Multi-Scale Models on Mesoscales and Squall Lines," Comm. Math. Sci., March 2010, Vol. 8, Issue, I, pp. 113-134
3. Y. Xing, A. Majda and W. Grabowski, "New Efficient Sparse Space-Time Algorithms for Superparameterization on Mesoscales," Mon. Wea. Rev., 2009, Vol. 137, Issue 12, pp. 4307-4323
4. A. Majda, "Multiscale Models with Moisture and Systematic Strategies for Superparameterization," J. Atmos. Sci., 2007, Vol. 64, pp. 2726-2734

# What is Superparameterization?

Attempt to Approximate Large Scale Behavior of Turbulent Anisotropic System without Large Scale gaps in Space-Time by a **much cheaper "on the fly"** algorithm with **imposed spectral gaps** but remains **statistically faithful** to the **large scale behavior**.

Kerstein – 1989 – Turbulent Mixing and Combustion
Grabowski and Smolarkiewicz – 1999, Grabowski – 2001, 2004 – MJO-like behavior

Geophysical Flows dominated by upscale transports from small scales (inverse cascades) of momentum, temperature, moisture, etc.

1. Moist convection on Mesoscales, Tropics, Midlatitudes
2. Mesoscale and Sub Mesoscale Eddies in Ocean
3. Gravity Wave Drag in Stratosphere

Challenge for Mathematicians:

Superparameterization needs mathematical numerical analysis statistical theory for behavior of such algorithms

| Superparameterization | HMM (E., Engquist, Vanden-Eijnden) |
|---|---|
| 1. Moderate Scale Gaps<br>$\epsilon$ = 1/6, 1/10 | 1. Large Scale Gaps<br>$\epsilon = 10^{-3}\ 10^{-6}\ 10^{-8}$ |
| 2. Small Scale behavior often does not have invariant measures | 2. Small Scale behavior has invariant measure |
| Skill relies on capturing statistical "intermittency" in space-time | Skill relies on efficient time integrators exploiting (1), (2) |

# Proposed framework for Superparameterization for Atmospheric, Oceanic, Engineering flows

(Majda, JAS, 2007; Majda and Grote, PNAS, 2009)

(i) Multi-scale formulation: A multi-scale physical/mathematical formulation (Klein, Majda, Stechmann, etc.)

(ii) Small-scale model: A mathematical model to represent the behavior of the smaller scales, typically involving a periodic spatial approximation and an imposed scale-gap.

(iii) Computational strategies to reduce the cost of the small scale models: Mathematical algorithms that allow for computationally efficient implementation of the small-scale model as a SP in a larger scale models. Small scale model solved in 1-Dor 2-D (Kerstein, Grabowski); Stochastic Models: Katsoulakis, Majda, Sopasakis; Khouider, Majda, Tropical Convection; Majda, Stechmann, CMT

# Mathematical test models for superparameterization

The test models posit the implicit separation of a physical system into its large scale slowly varying mean, u, and smaller scale more rapidly varying fluctuations, $u'$, akin to a Reynolds averaging formulation in turbulence. Here this is made explicit by introducing two spatial scales, X and x $\in \mathbb{R}^N$ with X = $\varepsilon$x, and two time scales t, $\tau$, with $\tau$ = t/$\varepsilon$ with $\varepsilon < 1$ a scale separation parameter. The physical field, U $\in \mathbb{R}^M$, then has the decomposition U = u(X, t)+$u'$ (X, $x$, t, $\tau$). The fluctuation $u'$ is always a zero mean Gaussian random field which is stationary in x for fixed (X, t, $\tau$) with Cov($u'$)(X, t, $\tau$) its M × M covariance matrix. For a function f (t, $\tau$),

$$< f > (t) = \varepsilon \int_0^{\varepsilon^{-1}} f(t,\tau)\, d\tau \quad [1]$$

denotes the empirical time average over the fluctuations for a fixed value of $\varepsilon$. Next, coupled equations for the large scale mean, u, and fluctuations $u'$are designed, with forms akin to those that occur in diverse complex physical applications. The large scale mean, $u$, in the test model is governed by the prototype **Large Scale Dynamics**

$$u_t + P\left(\frac{\partial}{\partial X}\right) u = F(< \mathrm{Cov}\,(u') >, \frac{\partial}{\partial X} < \mathrm{Cov}\,(u') >) + F_{ext}\,(X, t). \quad [2]$$

In [2], $F$, is in general a nonlinear function of its arguments which represents fluctuations in turbulent scalars such as moisture through the argument, Cov($u'$), and turbulent fluctuations from advection through the dependence on the gradient,$\frac{\partial}{\partial X}\, Cov(u')$. The quantity $F_{ext}$ is prescribed external forcing. We choose $P$ ($\frac{\partial}{\partial X}$) to be a fixed constant coefficient PDE of interest in the given physical context such as, for example, the hydrostatic primitive equations at a background rest state; clearly such test models develop non-trivial turbulent dynamics at the large scales only through the interaction with the statistics of the fluctuations. The prototype dynamics for the fluctuations u0 are given by the **Small Scale Dynamics**

$$u'_\tau + P'\left(u, \frac{\partial}{\partial X}\right) u' = -\sigma\,(x) W\,(x,\tau) + \Gamma\left(\frac{\partial}{\partial X}\right) u'.$$

## A Scalar Test Model for Superparametrization

Here, we develop the test model in detail in the simplest context for a real-valued scalar field, *u*, in a single-space dimension. The large-scale equations in **3** have the form,

$$\frac{\partial u}{\partial t} + P\left(\frac{\partial}{\partial X}\right) u = < \mathrm{Cov}(u') > (X,t) + F_{ext}$$

where $F_{ext}$ is a constant forcing. Here, the scalar differential operator $P\left(\frac{\partial}{\partial X}\right)$ is chosen to have advection, dispersion, and dissipation as in typical anisotropic systems in applications with

$$P\left(\frac{\partial}{\partial X}\right) = A\frac{\partial^3}{\partial X^3} - v\frac{\partial^2}{\partial X^2} + c\frac{\partial}{\partial X} + d.$$

The dispersion and advection coefficients are given the value $A = 1$, $c = 1$ while the viscosity and damping have the values $v = 10^{-8}$, $d = 10^{-2}$ in the simulations reported below. For the small-scale equations from **4** in their Fourier representation in **5**, we choose uniform damping, $\gamma k \equiv \gamma = 1$ and variance $\sigma_k^2$ to yield a $-\frac{5}{3}$ turbulent energy spectrum; in other words, $\sigma_k^2$ satisfies

$$\frac{\sigma_k^2}{2\gamma k} = \frac{E_0}{(|k|+1)^\beta} \qquad \beta = \frac{5}{3}$$

with the value $E_0 = 0.1$ for the preconstant. Thus, if the interaction with the large-scale field, *u*, is ignored in the equations for the small scales, the statistical equilibrium state is an energetic turbulent field without scale separation. A crucial design feature for the model is to build in intermittency by changing the large time behavior of the small-scale dynamic covariance equation in **8** as the value of *u* varies so that there are regions for *u* without statistical equilibration of the small-scale fluctuations. Here, we specify the symmetric part of $P_k'$ with the form (Diffusion and Anti-Diffusion )

$$\frac{P_k' + (P_k')^*}{2} = -f(u)A_k$$

With

$$f(u) = u\left(1 - \frac{u^2}{2}\right)$$

And

$$A_k = Ae^{-\partial|k|}|k|^2.$$

## Intermittency and Superparametrization in the Test Model

Here, we simulate the scalar test model as well as superparametrization with an imposed spatial scale gap defined by $L$ in Eq. **9** for a set of values of $L = 2, 1, 0.5$ in the regime of the test model with small-scale intermittency as described in detail in Eqs. **10**–**19** of the last section.We use the value $\varepsilon = 0.1$ with modest scale separation in the empirical time average from Eq. **2** needed in Eqs. **10** and **17**. The goal here is to explore the statistical accuracy of superparametrization in the test model in this regime with small-scale intermittency and modest scale separation mimicking realistic physical systems.

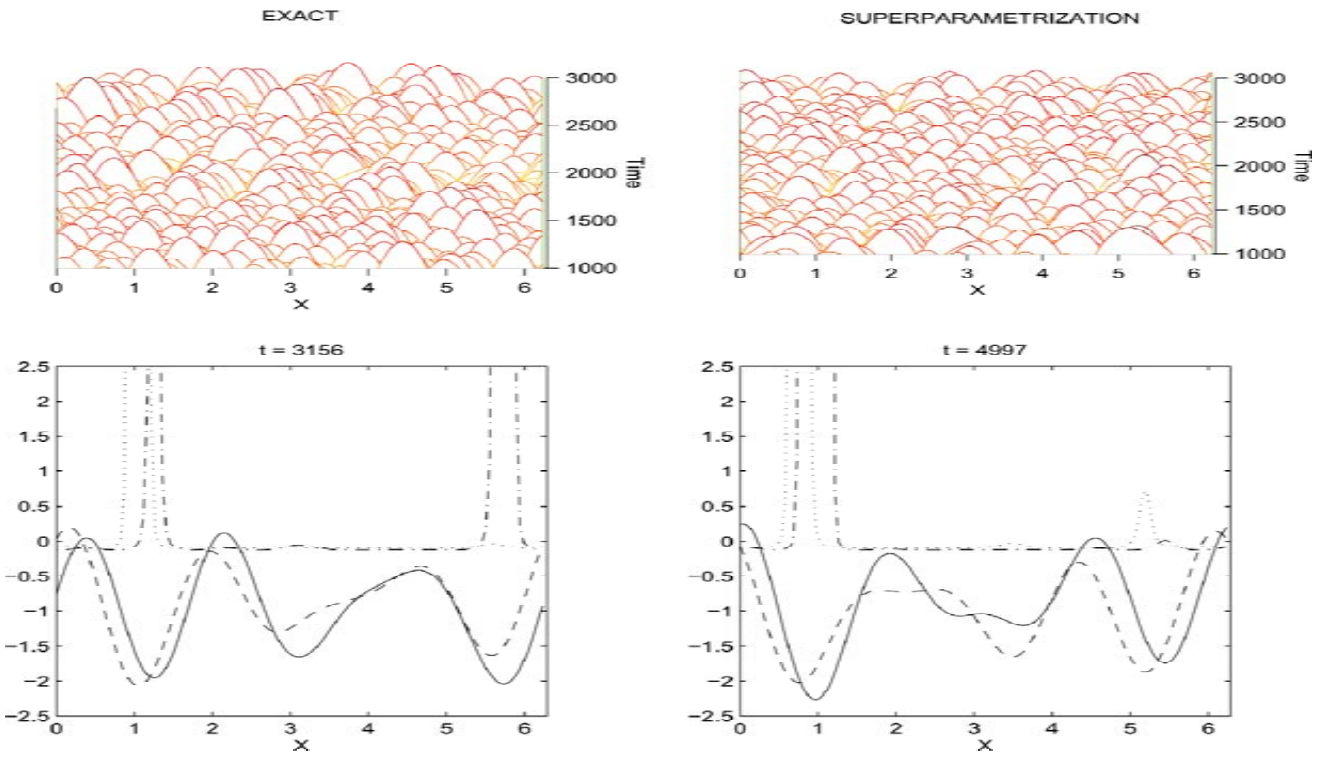

# PART II

# New Multi-Scale Models on Mesoscales and Squall Lines

*Andrew J. Majda*
and
*Yulong Xing*

# Introduction

- We develop new multi-scale models on the mesoscale and microscales which provide potentially new insight into the multi-scale development of organized squall lines on mesoscales.

microscales $L_m = 10\,\mathrm{km}, \qquad T_m = 15\,\mathrm{min}.$

mesoscale $L_M = 100\,\mathrm{km} = \epsilon^{-1} L_m, \qquad T_M = 2.5\,\mathrm{hrs} = \epsilon^{-1} T_m$

# Introduction

We show that

- upright single mode convective heating without tilts can lead to significant upscale convective momentum transport from the microscales to the mesoscales due to the strong shear.

- self-similarity in squall line dynamics exists as the ambient shear strength changes.

# Tropical Squall Lines

Moist nonhydrostatic anelastic equations with bulk cloud microphysics:

$$
\begin{aligned}
\frac{D\mathbf{u}_h}{Dt} &= -\nabla_h p \\
\frac{Dw}{Dt} &= -p_z + \epsilon^{-1}\theta + (\bar{\epsilon} q_v - q_r - q_c) \\
\frac{D\theta}{Dt} + N^2(z)\epsilon^{-1} w &= \epsilon^{-1} L \frac{\theta_0}{p_0}(C_d - E_r) \\
div_h \mathbf{u}_h + \rho^{-1}(\rho w)_z &= 0, \\
\frac{Dq_v}{Dt} &= -C_d + E_r \\
\frac{Dq_c}{Dt} &= C_d - A_r \\
\frac{Dq_r}{Dt} - \frac{1}{\rho}\frac{\partial}{\partial z}(\rho V_t q_r) &= A_r - E_r.
\end{aligned}
$$

with $\dfrac{D}{Dt} = \dfrac{\partial}{\partial t} + \mathbf{u}_h \cdot \nabla_h + w\dfrac{\partial}{\partial z},$

and the space-time scales

$$L_m = 10\,\mathrm{km} \qquad \text{and} \qquad T_m = 15\,\mathrm{min}, \qquad [\mathbf{u}_h] = [w] = 10\,\mathrm{m/s},$$

# Tropical Squall Lines

$\mathbf{u}_h = (u, v)$ Horizontal velocities

$w$ Vertical velocity

$\rho(z), N^2(z), \theta_0(z), p_0(z)$ the non-dimensional form of the dry statically stable vertical profile

$\theta$ potential temperature

$p$ Pressure

$L$ Latent heat prefactor

The quantities $q_v$ , $q_c$ , $q_r$ are the mixing ratios for cloud vapor, water, and rain, respectively, rescaled by the factors $\varepsilon^{-2}$, $\varepsilon^{-2}$, $\varepsilon^{-2}$, respectively.

$C_d$ Condensation of cloud vapor

$E_r$ Evaporation of rain

$A_r$ Conversion of cloud water to rain by both autoconversion and collection

$V_T$ Fall velocity

# Tropical Squall Lines

Non-dimensional units are used with the following reference scales:

| Parameter | Nondimensional reference units | Description |
|---|---|---|
| L | 10 km | length scale |
| t | 15 min | time scale |
| u,w | 10 km/15 min $\approx$ 10 m/s | horizontal and vertical velocity scale |
| $\theta$ | 3 K | potential temperature scale |

# Tropical Squall Lines

The squall line experiment designed in [Grabowski 2006] is explored:

- 2D version of moist nonhydrostatic anelastic equations with 1024 km length and 25 km height.
- The initial temperature, humidity profiles and horizontal wind fields are based on the GARP GATE Phase-III mean sounding.
- A 4-km-deep, 512-km-long cold pool of $D\theta = -6.75$ K and $Dq_v = -3.5$ g kg$^{-1}$ is placed in the domain on the initial data to initiate convection.
- Impose a large-scale forcing representing climatological background through the cooling and moistening rates for the first 6 hours, then remove it.
- A 10% amplitude random noise is added to the surface fluxes to provide small-scale excitation (important for the initial development of convection).

# Tropical Squall Lines

Three different initial large scale background shears are used:

$$\bar{U}(z) = \begin{cases} a(\cos(\frac{\pi z}{1.2}) - \cos(\frac{2\pi z}{1.2})) & \text{if } z < 1.2, \\ -2a & \text{otherwise.} \end{cases}$$

with a = 1, 0.8 and 0.5.

The steering level:

height where the phase speed is equal to the squall line flow speed of the emerging wave.

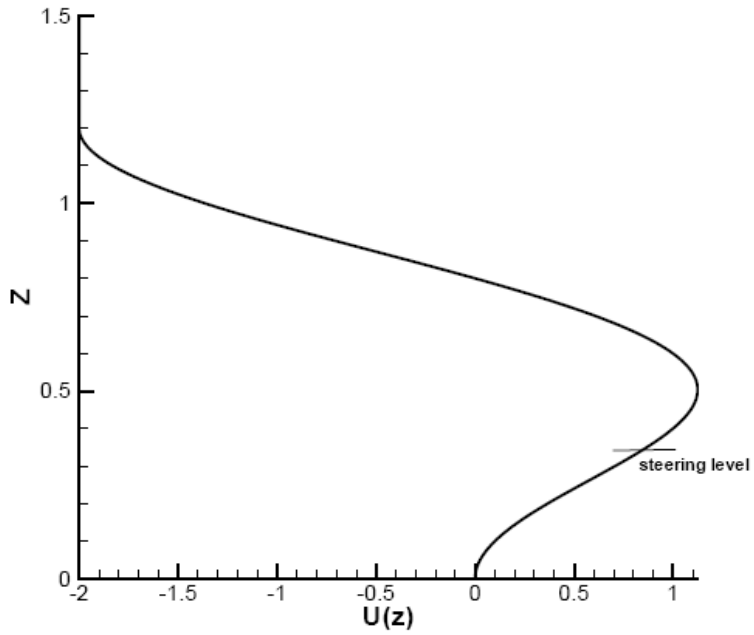

# Tropical Squall Lines

The stopping time is set as 36 hours, when the squall line remains statistically steady for a long time.

We show the velocity of the steering level (also noted as squall line speed),
and the maximum of the original background shear before we subtract the squall line speed, defined as jet max.

| Experiment | a=1 | a=0.8 | a=0.5 |
|---|---|---|---|
| Jet max | 1.125 | $0.9 = 1.125 \times a$ | $0.5625 = 1.125 \times a$ |
| Squall line speed | 0.825 | $0.66 = 0.825 \times a$ | $0.4125 = 0.925 \times a$ |
| Steering level (height) | 0.34 | 0.34 | 0.34 |

We observe:
a propagating squall line always emerges in these three cases with speed determined by the exactly same steering level

# Tropical Squall Lines

The time averaged numerical solution of horizontal velocity is denoted by $\langle \bar{u} \rangle$, Thus the large scale velocity, on mesoscales of order 100 km or 10 in nondimensional units, is defined as

$$\langle \bar{u} \rangle(x) = \frac{1}{9.6} \int_{-4.8}^{4.8} \langle u \rangle(x+s) ds,$$

and the spatial fluctuation is

$$\langle u' \rangle(x) = \langle u \rangle(x) - \langle \bar{u} \rangle(x).$$

# Tropical Squall Lines

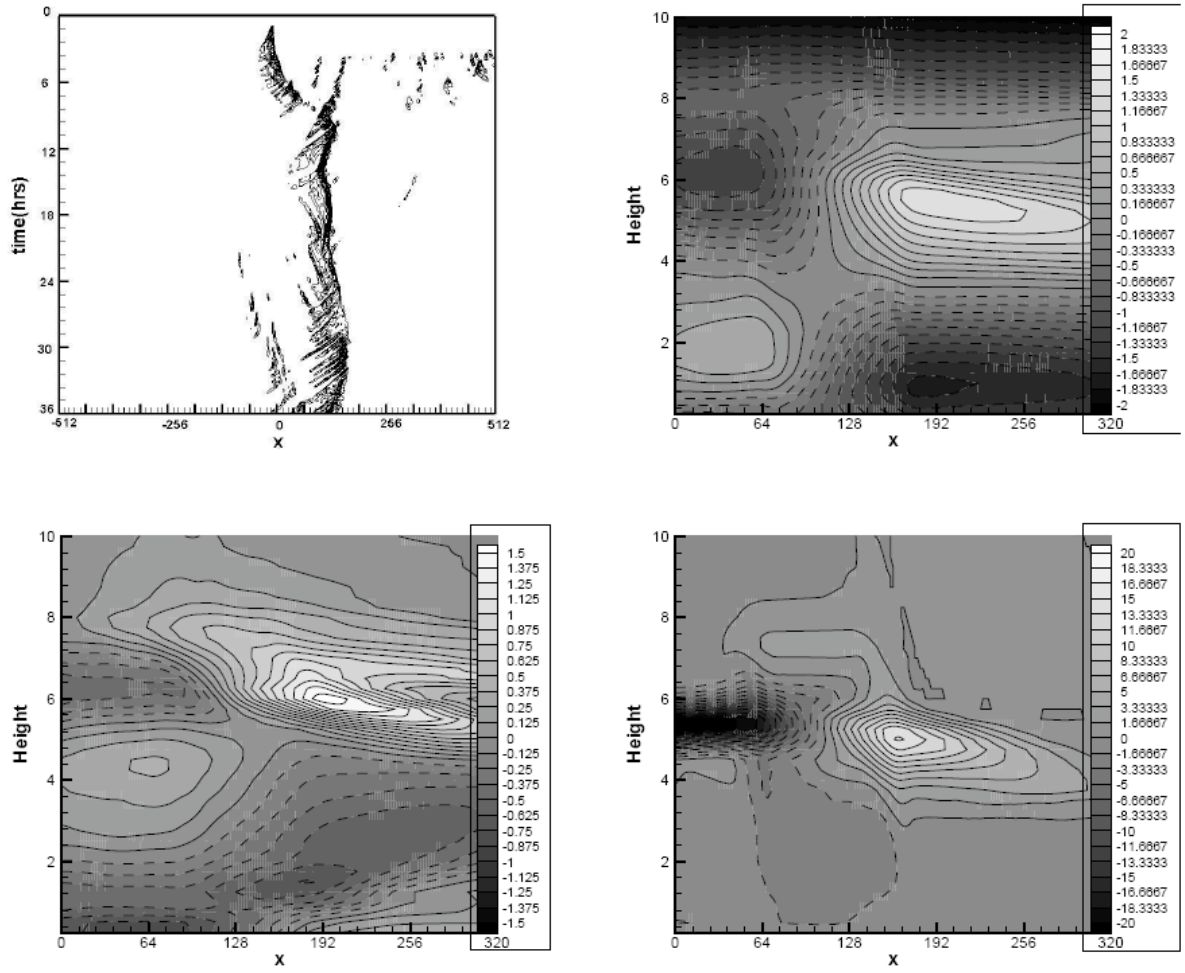


Figure 3: The contours of the variables from the squall-line simulation with $a = 1$. Top left: Surface precipitation; Top right: Large scale horizontal velocity $\langle \bar{u} \rangle$; Bottom left: Large scale potential temperature $\langle \bar{\theta} \rangle$; Bottom right: Large scale source term $\langle \bar{S}_\theta \rangle$. Note: 1, the units for x-axis and height are both km in these plots, rather that the non-dimensional units; 2, solid contour line represents positive value and dashed one represents negative value.

# Tropical Squall Lines

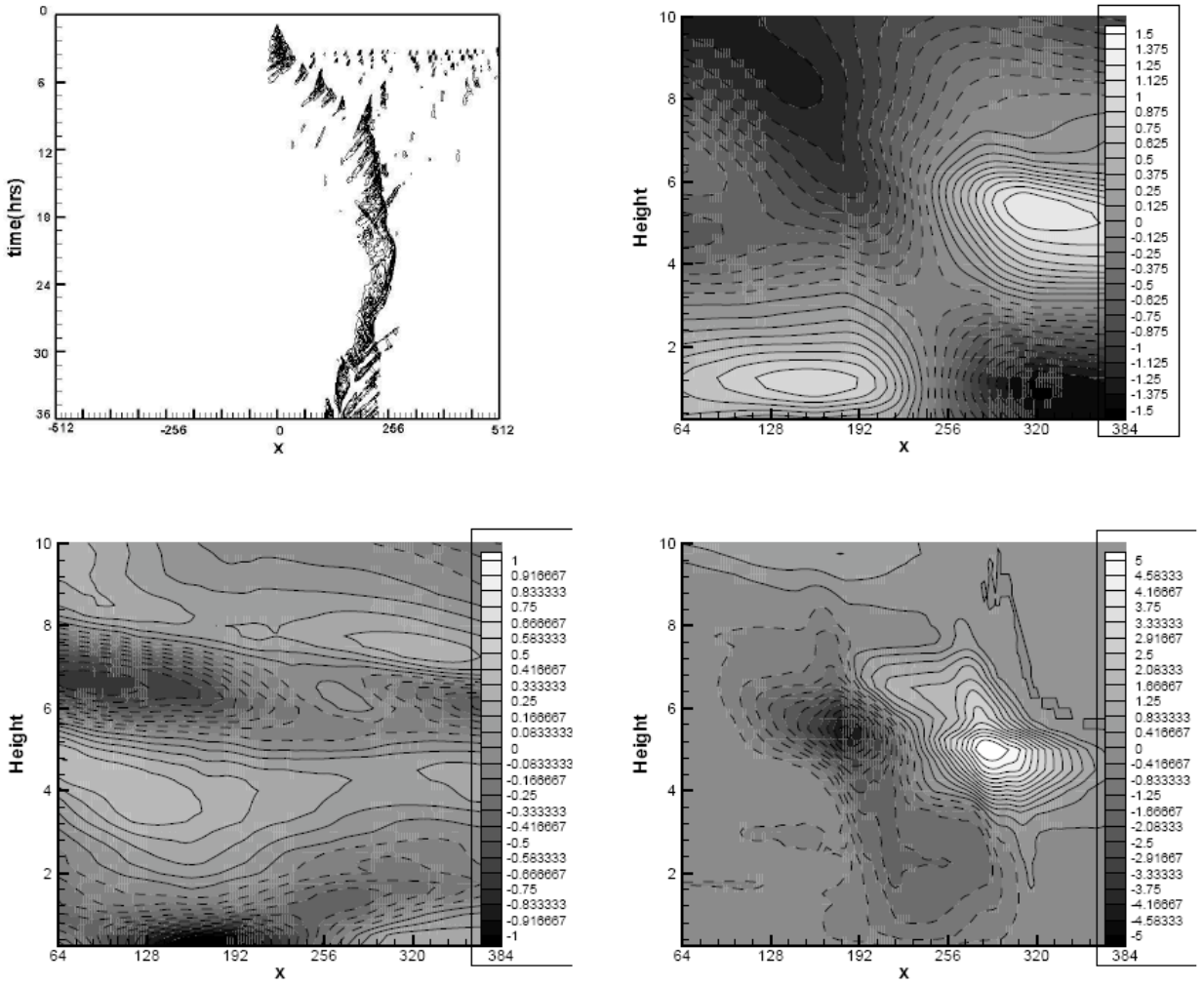


Figure 5: The contours of the variables from the squall-line simulation with $a = 0.5$. Top left: Surface precipitation; Top right: Large scale horizontal velocity $\langle \bar{u} \rangle$; Bottom left: Large scale potential temperature $\langle \bar{\theta} \rangle$; Bottom right: Large scale source term $\langle \bar{S}_\theta \rangle$. Note: 1, the units for x-axis and height are both km in these plots, rather that the non-dimensional units; 2, solid contour line represents positive value and dashed one represents negative value.

# Tropical Squall Lines

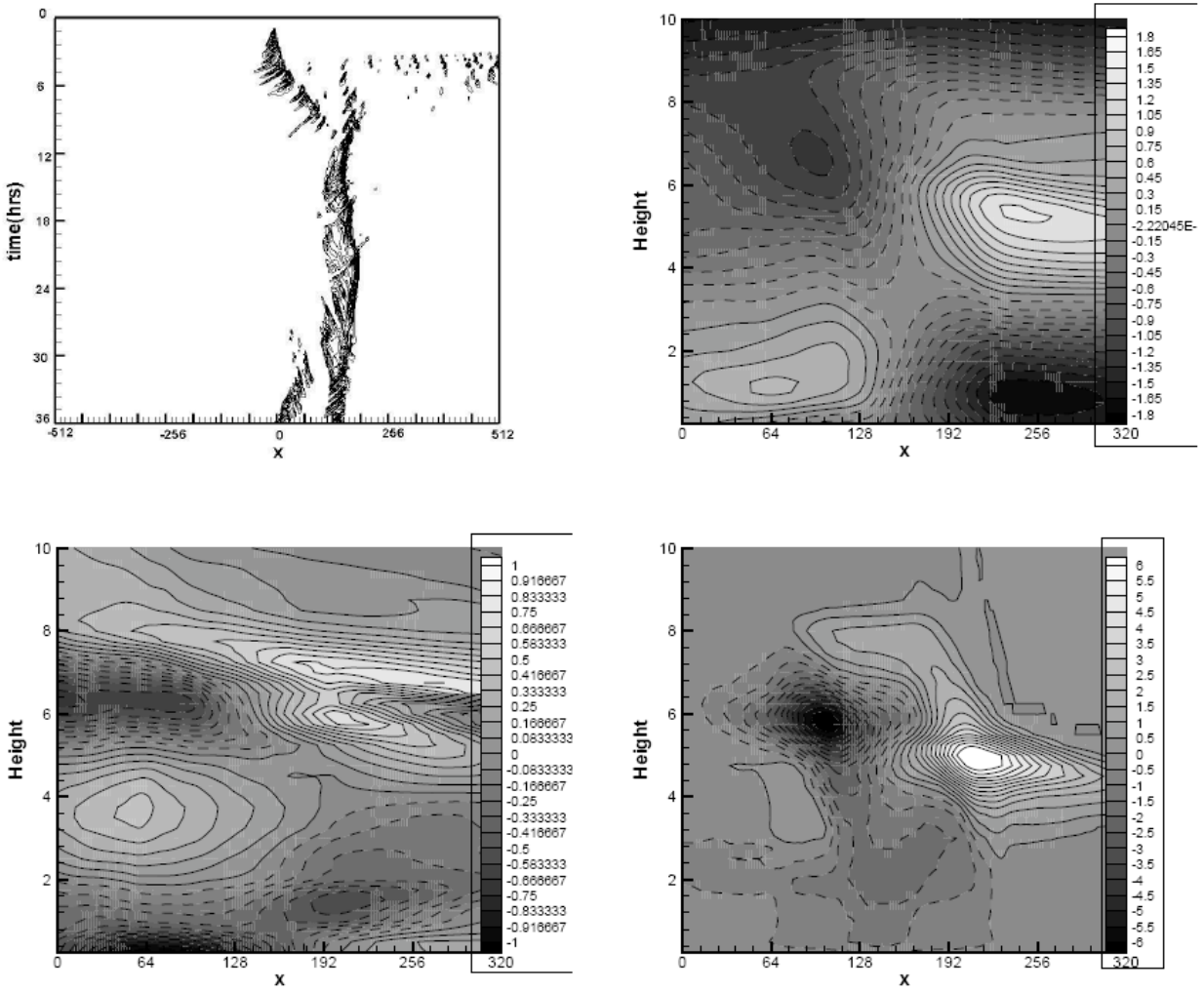


Figure 4: The contours of the variables from the squall-line simulation with $a = 0.8$. Top left: Surface precipitation; Top right: Large scale horizontal velocity $\langle \bar{u} \rangle$; Bottom left: Large scale potential temperature $\langle \bar{\theta} \rangle$; Bottom right: Large scale source term $\langle \bar{S}_\theta \rangle$. Note: 1, the units for x-axis and height are both km in these plots, rather that the non-dimensional units; 2, solid contour line represents positive value and dashed one represents negative value.

# Tropical Squall Lines

Large scale horizontal velocities have very similar structures,
due to the fact that the initial background shears share the same structure.

The horizontal velocity has a shock-like structure with strong negative velocities at low levels in front but at high levels behind the squall line, i.e. a jump updraft.

We compute the correlation between these plots after a phase shift aligning the center of the squall lines. Large scale variables' structures are not affected by altering the strength of the background shears only and are qualitatively self-similar.

Table 2: The correlation between the large scale variables from these simulations.

| | Between experiments a=1 and a=0.8 | Between experiments a=1 and a=0.5 |
|---|---|---|
| $\langle \bar{u} \rangle$ | 0.9278 | 0.8923 |
| $\langle \bar{\theta} \rangle$ | 0.9002 | 0.8579 |
| $\langle S_\theta \rangle$ | 0.8972 | 0.8431 |

# Tropical Squall Lines

If the shear becomes sufficiently weak, i.e. a is small enough ,
the turbulent travelling wave will decay and not propagate in time.

Conclusion:

Even in a thermodynamic background favorable for the formation of a squall line, a weak enough background shear flow does not generate a squall line

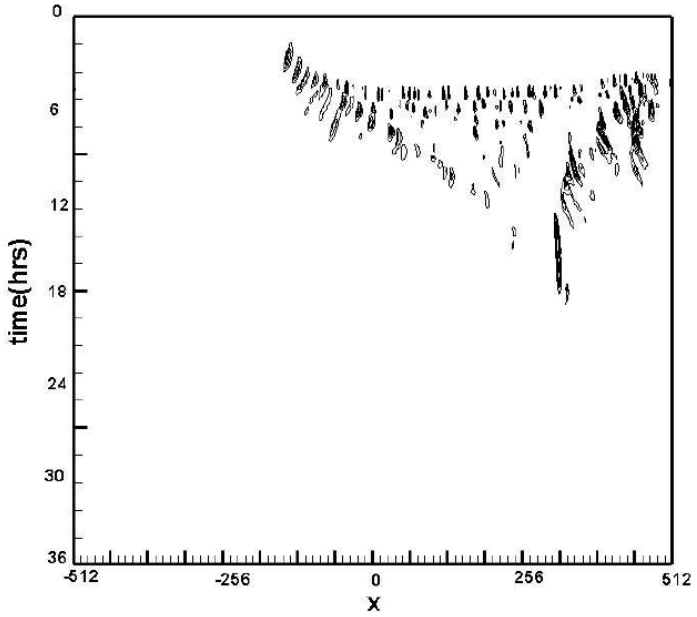


Figure 6: The contours of surface precipitation from the squall-line simulation with $a = 0.3$.

# Tropical Squall Lines

We then show the data: $\overline{(\langle w' \rangle \langle u' \rangle)_z}$, $\overline{(\langle w' \rangle \langle \theta' \rangle)_z}$, $\langle S'_\theta \rangle$ and $\langle S'_w \rangle$

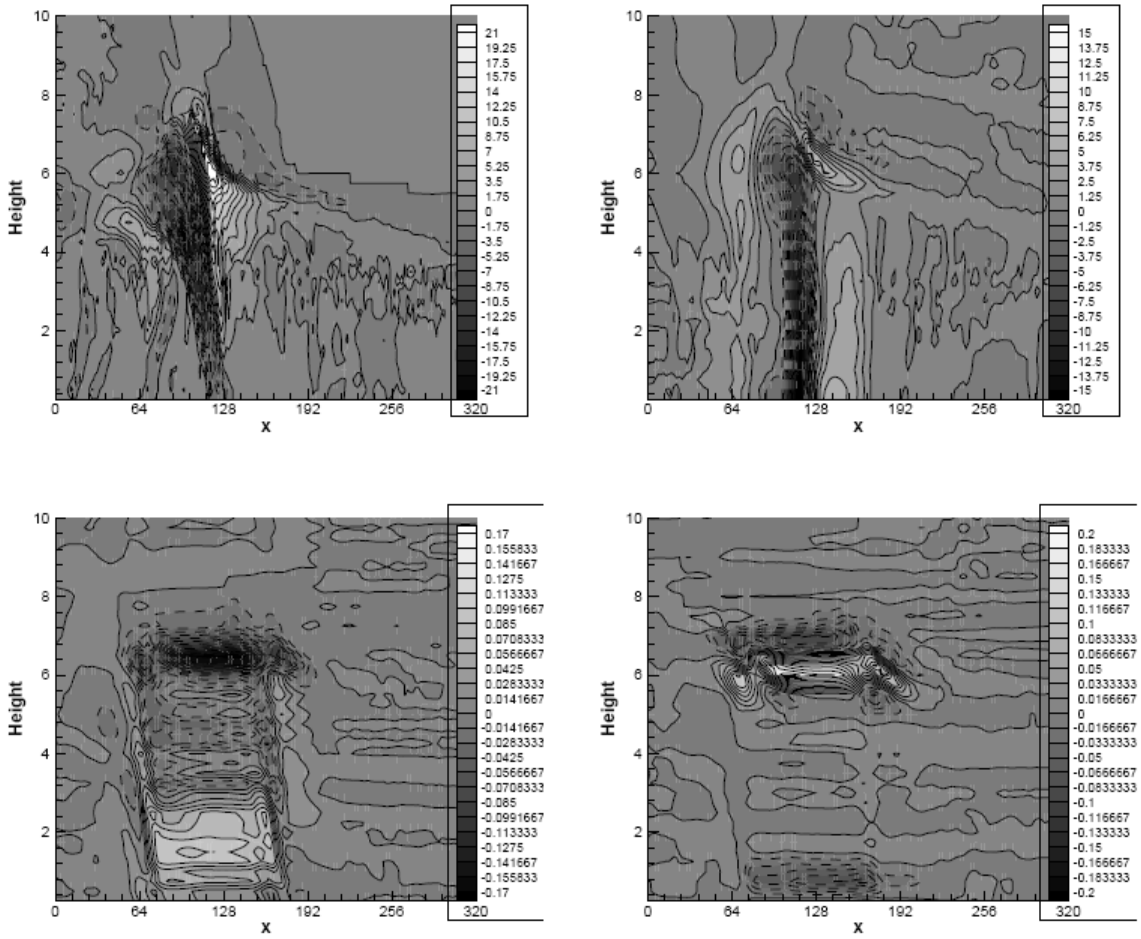


Figure 7: The contours of the variables from the squall-line simulation with $a = 1$. Top left: Source term fluctuation $\langle S'_\theta \rangle$; Top right: Source term fluctuation $\langle S'_w \rangle$; Bottom left: The eddy flux $\overline{(\langle u' \rangle \langle w' \rangle)_z}$; Bottom right: The eddy flux $\overline{(\langle w' \rangle \langle \theta' \rangle)_z}$. Note: 1, the units for x-axis and height are both km in these plots, rather that the non-dimensional units; 2, solid contour line represents positive value and dashed one represents negative value.

# PART III

# New Efficient Sparse Space-Time Algorithms for Superparameterization on Mesoscales

YULONG XING * , ANDREW J. MAJDA

*Department of Mathematics and Climate, Atmosphere and Ocean Science*

*Courant Institute of Mathematical Sciences*

*New York University, New York, NY, 10012*

WOJCIECH W. GRABOWSKI

*National Center for Atmospheric Research*

*Boulder, Colorado, 80307*

Y. Xing, A.J. Majda and W.W. Grabowski, *New efficient sparse space-time algorithms for superparameterization on mesoscales,* ***Monthly Weather Review***, v137 (2009), pp.4307-4324

# Superparameterization (SP)

## Why Superparameterization?

SP is ideally suited for parallel computers and can operate with one to two orders of magnitude fewer computations than a 3D cloud-resolving large-scale model.

## What is Superparameterization?

Represent subgrid scales of the 3D large scale model (of 100s km resolution ) by embedding **periodic** domain **2D** CRM (resolution around 1 km) in each column of the large scale model.

Also referred as Cloud-Resolving Convection Parameterization (CRCP).

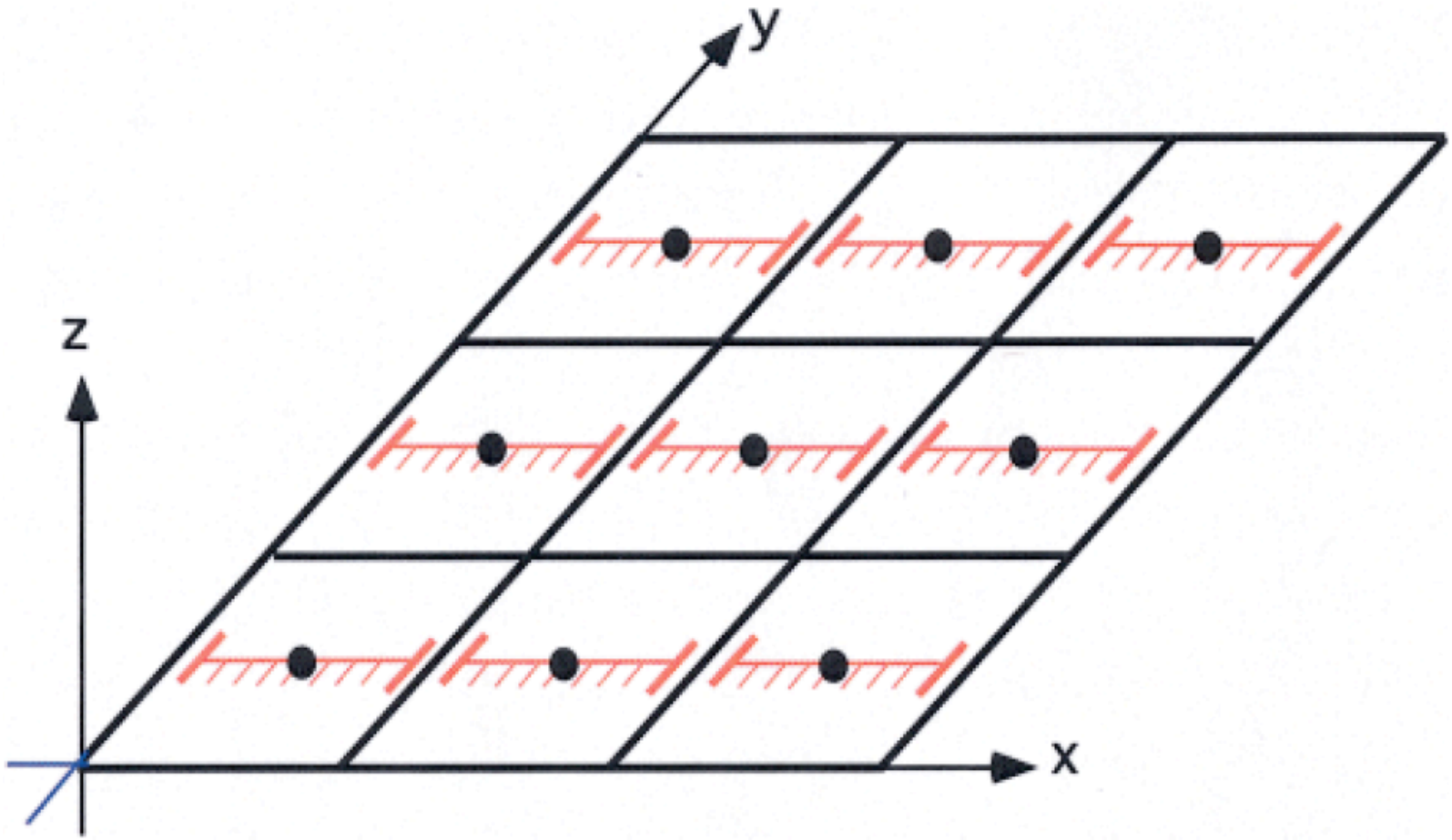


**The black squares represent an array of GCM grid boxes, and the red lines represent embedded two dimensional CRMs.**

# Details of SP

The anelastic equations of the cloud-scale model are as follows:

$$\frac{d\mathbf{u}}{dt} = -\nabla'\pi + \mathbf{k}gb + \mathbf{i}(s_u + f_{\mathrm{LS}}^{u}) + d_{\mathbf{u}}$$

$$\nabla' \cdot (\rho_o \mathbf{u}) = 0$$

$$\frac{d\theta}{dt} = \frac{\theta_e}{T_e}\left[\frac{L_v}{c_p}(\mathrm{CON} + \mathrm{DEP}) + r\right] + s_\theta + f_{\mathrm{LS}}^{\theta} + d_\theta$$

$$\frac{dq_v}{dt} = -\mathrm{CON} - \mathrm{DEP} + s_{q_v} + f_{\mathrm{LS}}^{q_v} + d_{q_v}$$

$$\frac{dq_c}{dt} = \mathrm{CON} - \mathrm{ACC} - \mathrm{AUT} + f_{\mathrm{LS}}^{q_c} + d_{q_c}$$

$$\frac{dq_p}{dt} = \frac{1}{\rho_o}\frac{\partial}{\partial z}(\rho_o v_t q_p) + \mathrm{ACC} + \mathrm{AUT} + \mathrm{DEP} + f_{\mathrm{LS}}^{q_p} + d_{q_p},$$

where $d/dt \equiv \partial/\partial t + \mathbf{u} \cdot \nabla'$ with $\nabla' \equiv (\partial/\partial x, \partial/\partial z)$

The lowercase symbols have the same meaning as the respective uppercase symbols in large scale system.

# Details of SP

Denote the large scale variables by:

$$Q = Q\,(X, Y, z, t)$$

the small scale variables by:

$$q = q\,(x, z, t)\,|_{(X,Y)}$$

The fundamental property of the two sets of variables

$$Q\,(X, Y, z, t) = <\, q\,(x, z, t)\,|_{(X,Y)}\,>$$

Horizontal averaging of a cloud scale dependent variable:

$$\langle q(x,\ z,\ t)|_{(X,Y)}\rangle \equiv \frac{1}{L}\int_{-L/2}^{L/2} q(\xi,\ z,\ t)|_{(X,Y)}\ d\xi,$$

# Numerical algorithm

## Large-scale model equations

$$\frac{\partial Q}{\partial t} = A_Q + S_Q + F_{CS}^Q$$

where $A_Q \equiv -\mathbf{U} \cdot \boldsymbol{\nabla} Q$ is the large-scale advection term

## Small-scale model equations

$$\frac{\partial q}{\partial t} = a_q + s_q + f_{\mathrm{LS}}^q$$

where $a_q \equiv -\mathbf{u} \cdot \boldsymbol{\nabla} q$ ($\mathbf{u}$ is the small-scale flow)

# Numerical algorithm

The algorithm proceeds from time level *n* to *n* + 1 over the large-scale model time step $\Delta T$ as follows: ($N\Delta t = \Delta T$ )

1. The large scale model is solved from T to T + $\Delta T$

$$Q|^{n+1} = Q|^{n} + \Delta T(A_Q + S_Q)|_n^{n+1} + \Delta T F_{CS}^{Q}|^{n},$$

2. Define the large scale forcing to small scale as

$$f_{LS}^{q}|^{n} = \frac{Q|^{n+1} - \langle q|^{n}\rangle}{\Delta T},$$

and the small scale models are solved from T to T+ $N\Delta t$ by

$$\langle q|^{n+1}\rangle = \langle q|^{n}\rangle + \sum_{i=1}^{N} \Delta t(a_q + s_q)|_i^{i+1} + \sum_{i=1}^{N} \Delta t f_{LS}^{q}|^{n}.$$

3. Define the small scale feedback as:

$$F_{CS}^{Q}|^{n+1} = \frac{\langle q|^{n+1}\rangle - Q|^{n+1}}{\Delta T},$$

which ensures the relation: Q = < q >.

# Reduced time strategy

The small scale model is solved over the whole time, as $\Delta T = N\Delta t$

Contribution of small scale model to large scale model :

$$F_{CS}^{Q}$$

We can solve the small scale model for part of the time interval and find an approximate estimation of it.

Idea: Solve the small scale model for N/p small scale time steps instead of N small scale time steps, for an arbitrary constant p.

# Reduced time strategy

1. The large scale model is unchanged:

$$Q|^{n+1} = Q|^n + \Delta T(A_Q + S_Q)|_n^{n+1} + \Delta T F_{CS}^Q|^n,$$

2. Define the large scale forcing to small scale as

$$f_{LS}^q = \frac{Q|^{n+1} - \langle q|^n \rangle}{\Delta T/p} = p\frac{Q|^{n+1} - \langle q|^n \rangle}{\Delta T},$$

and the small scale models are solved from T to T+ $\frac{N}{p}\Delta t$ by

$$\langle q|^{n+\frac{1}{p}} \rangle = \langle q|^n \rangle + \sum_{i=1}^{N/p} \Delta t(a_q + s_q)|_i^{i+1} + \sum_{i=1}^{N/p} \Delta t f_{LS}^q.$$

$q|^{n+1}$? The simple approximation $q|^{n+1} = q|^{n+\frac{1}{p}}$ are employed.

3. Define the small scale feedback as:

$$F_{CS}^Q|^{n+1} = \frac{\langle q|^{n+1} \rangle - Q|^{n+1}}{\Delta T} = \frac{\langle q|^{n+\frac{1}{p}} \rangle - Q|^{n+1}}{\Delta T}.$$

# Reduced space strategy

Can the computational cost be saved spatially?

In the original superparameterization, the large scale domain is divided into grids with horizontal size $\Delta X$, which is also assigned to be the domain of each small scale simulation.

We keep the large scale cell size be $\Delta X$
let the horizontal domain of the small scale model be $\Delta X/p$
for arbitrary p

# Reduced space strategy

The large scale forcing and small scale feedback keep the same formula, but the spatial average is over $\Delta X/p$ domain:

$$f_{LS}^{q} = \frac{Q|^{n+1} - \langle q|^{n} \rangle}{\Delta T},$$
$$F_{CS}^{Q}|^{n+1} = \frac{\langle q|^{n+1} \rangle - Q|^{n+1}}{\Delta T}.$$

# Reduced time and space strategy

Combine those two strategies together, to save both time and spatial computational costs.

- Solve the large scale model first by

$$Q|^{n+1} = Q|^n + \Delta T(A_Q + S_Q)|_n^{n+1} + \Delta T F_{CS}^Q|^n.$$

- Define the new large scale forcing, with the spatial average over $\Delta X/p$ domain

$$f_{LS}^q = \frac{Q|^{n+1} - \langle q|^n \rangle}{\Delta T/p} = p\frac{Q|^{n+1} - \langle q|^n \rangle}{\Delta T}.$$

- Solve the small scale model by

$$\langle q|^{n+\frac{1}{p}} \rangle = \langle q|^n \rangle + \sum_{i=1}^{N/p} \Delta t(a_q + s_q)|_i^{i+1} + \sum_{i=1}^{N/p} \Delta t f_{LS}^q.$$

- Assume $q|^{n+1} = q|^{n+\frac{1}{p}}$, and define the small scale feedback as

$$F_{CS}^Q|^{n+1} = \frac{\langle q|^{n+1} \rangle - Q|^{n+1}}{\Delta T} = \frac{\langle q|^{n+\frac{1}{p}} \rangle - Q|^{n+1}}{\Delta T},$$

with the spatial average over $\Delta X/p$ domain.

# Reduced time and space strategy

Assume 1/p small scale time steps and spatial cells are both employed, the computational cost of small scale model is decreased by $1/p^2$.

We denote the new efficient algorithms by

Sparse Space-Time algorithms for SuperParameterization (SSTSP).

# An alternative formula of the algorithm

Switching the order to solve large and small scale models.

Original SP becomes:

1. The small scale model is solved from T to $T + N\Delta t = T + \Delta T$

$$\langle q|^{n+1}\rangle = \langle q|^{n}\rangle + \sum_{i=1}^{N} \Delta t(a_q + s_q)|_i^{i+1} + \sum_{i=1}^{N} \Delta t f^q_{LS,SO}|^n,$$

2. Define the small scale feedback as:

$$F^Q_{CS,SO}|^n = \frac{\langle q|^{n+1}\rangle - Q|^n}{\Delta T}.$$

and the large scale models are solved from T to T+ $\Delta T$ by

$$Q|^{n+1} = Q|^n + \Delta T(A_Q + S_Q)|_n^{n+1} + \Delta T F^Q_{CS,OS}|^n,$$

3. Define the large scale forcing to small scale as

$$f^q_{LS,OS}|^{n+1} = \frac{Q|^{n+1} - \langle q|^{n+1}\rangle}{\Delta T}$$

Comparable numerical results are obtained by the two forms of SP.

# An alternative formula of the algorithm

SSTSP becomes:

1. The small scale model is solved from T to T+ $\frac{N}{p}\Delta t$

$$\langle q|^{n+\frac{1}{p}}\rangle = \langle q|^{n}\rangle + \sum_{i=1}^{N/p}\Delta t(a_q + s_q)|_i^{i+1} + \sum_{i=1}^{N/p}\Delta t f^q_{LS,OS}|^n,$$

2. Define the small scale feedback as: (by assuming $q|^{n+1} = q|^{n+\frac{1}{t}}$)

$$F^Q_{CS,OS}|^n = \frac{\langle q|^{n+\frac{1}{p}}\rangle - Q|^n}{\Delta T/p} = p\frac{\langle q|^{n+1}\rangle - Q|^n}{\Delta T}.$$

and the large scale models are solved from T to T+ $\Delta T$ by

$$Q|^{n+1} = Q|^n + \Delta T(A_Q + S_Q)|_n^{n+1} + \Delta T F^Q_{CS,OS}|^n,$$

3. Define the large scale forcing to small scale as

$$f^q_{LS,OS}|^{n+1} = \frac{Q|^{n+1} - \langle q|^{n+1}\rangle}{\Delta T}$$

# An alternative formula of the algorithm

Two main changes, compared with SP :

a) $q|^{n+1} = q|^{n+\frac{1}{p}}$

b) $F^{Q}_{CS,OS}|^{n} = \dfrac{\langle q|^{n+\frac{1}{p}}\rangle - Q|^{n}}{\Delta T/p} = p\dfrac{\langle q|^{n+1}\rangle - Q|^{n}}{\Delta T}$

is p times bigger.

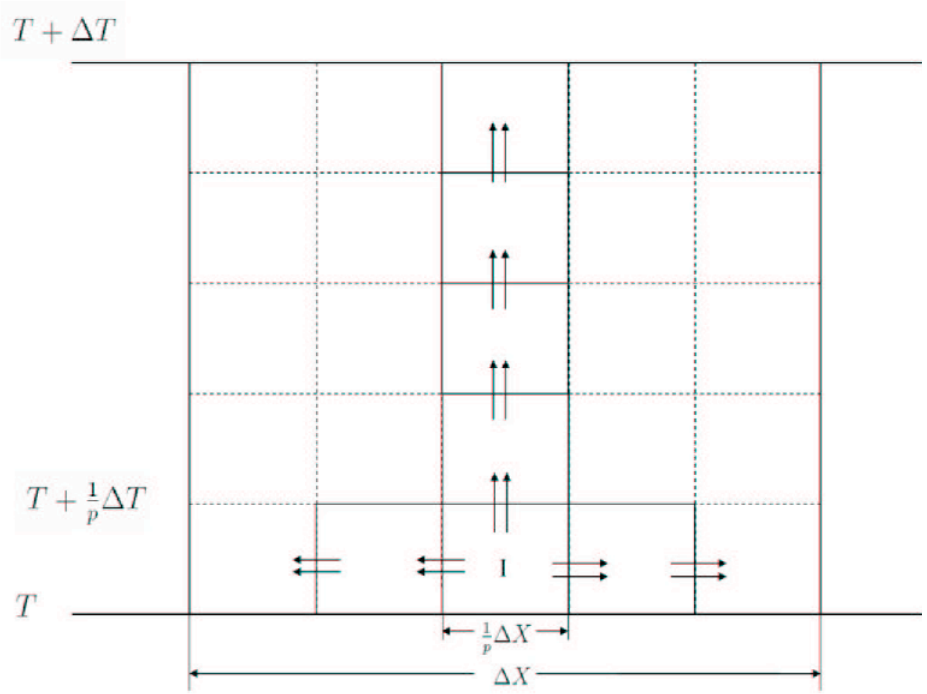


One explanation :

periodically extend the solution inside I to the big domain.

# An alternative formula of the algorithm

To be consistent with the original SP,
the first approach is used in the following tests.

This alternative algorithm gives comparable performance on all the tests.

# Squall line experiment setup

The 2D squall line experiment designed in [Grabowski 2006] is explored:

- 2D domain of 1024 km length and 25 km height.
- The initial temperature, humidity profiles and horizontal wind fields are based on the GARP GATE Phase-III mean sounding.
- A 4-km-deep, 512-km-long cold pool of $D\theta = -6.75$ K and $Dq_v = -3.5$ g kg$^{-1}$ is placed in the domain on the initial data to initiate convection.
- Impose a large-scale forcing representing climatological background through the cooling and moistening rates for the first 6 hours, then remove it.
- A 10% amplitude random noise is added to the surface fluxes to provide small-scale excitation (important for the initial development of convection).

# Test bed

The following initial large scale background shears are used:

$$\bar{U}(z) = \begin{cases} 10a(cos(\frac{\pi z}{12}) - cos(\frac{2\pi z}{12})) & \text{if } z < 12, \\ -20a & \text{otherwise.} \end{cases}$$

with a = 1, 0.8, 0.5, 0.3.

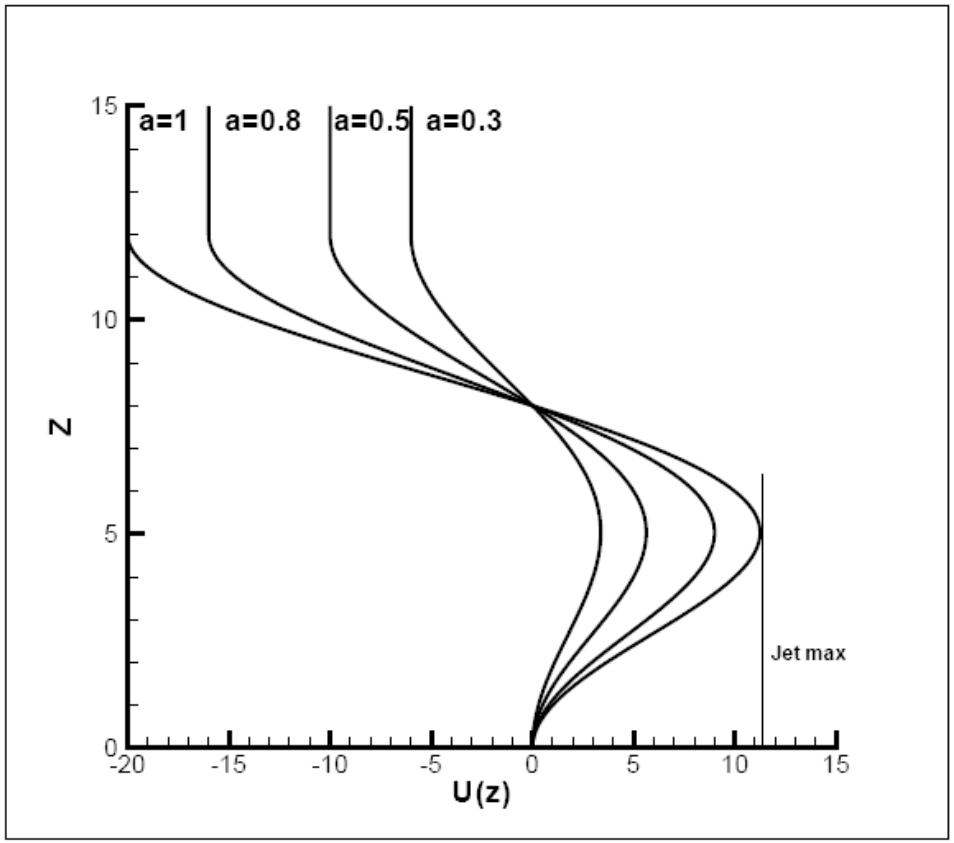

# Test bed

a = 1, 0.8, 0.5: (strong or weak shear)

Propagating squall line emerges in these three cases.

a = 0.3: (weaker shear)

Dying scattered convection. No squall line is generated.

# Application to squall lines

Five simulations:

- CRM: Cloud-Resolving Model
- SP: Original superparameterization simulation
- SSTSP2: Efficient algorithm with p=2
- SSTSP3: Efficient algorithm with p=3
- SSTSP6: Efficient algorithm with p=6

# Application to squall lines

Setup for these simulations:

CRM: resolution ~ 1km, time step ~ 10 seconds.

SP, SSTSP2, SSTSP3, SSTSP6:
large scale horizontal domain size 1024 km with resolution 32 km
large time step ~ 60 seconds, small time step ~ 10 seconds.

SP: small scale horizontal domain size 32 km with resolution 1 km
small time models are solved 6 times in each large time step

SSTSP2: small scale horizontal domain size 16 km with resolution 1 km
small time models are solved 3 times in each large time step

SSTSP3: small scale horizontal domain size 10 km with resolution 1 km
small time models are solved 2 times in each large time step

SSTSP6: small scale horizontal domain size 6 km with resolution 1 km
small time models are solved 1 time in each large time step

# Application to squall lines

The stopping time is set as 36 hours, when the squall line remains statistically steady for a long time.

We show the jet max and mean propagation speed of the squall line:

| | CRM | SP | SSTSP2 | SSTSP3 | SSTSP6 |
|---|---|---|---|---|---|
| Jet max(km) | 11.25 | 11.25 | 11.25 | 11.25 | 11.25 |
| Mean propagation speed (m/s) | 8.25 | 8.25 | 8.25 | 8.25 | 8.25 |

Mean propagation speed keeps the same for all these five experiments.

Mean propagation speed is subtracted from the initial background shear, so the squall line stays near the center.

Fig 1. The contours of the surface precipitation when a=1.
Top left: CRM; Top right: SP; Bottom left: SSTSP3; Bottom right: SSTSP6.

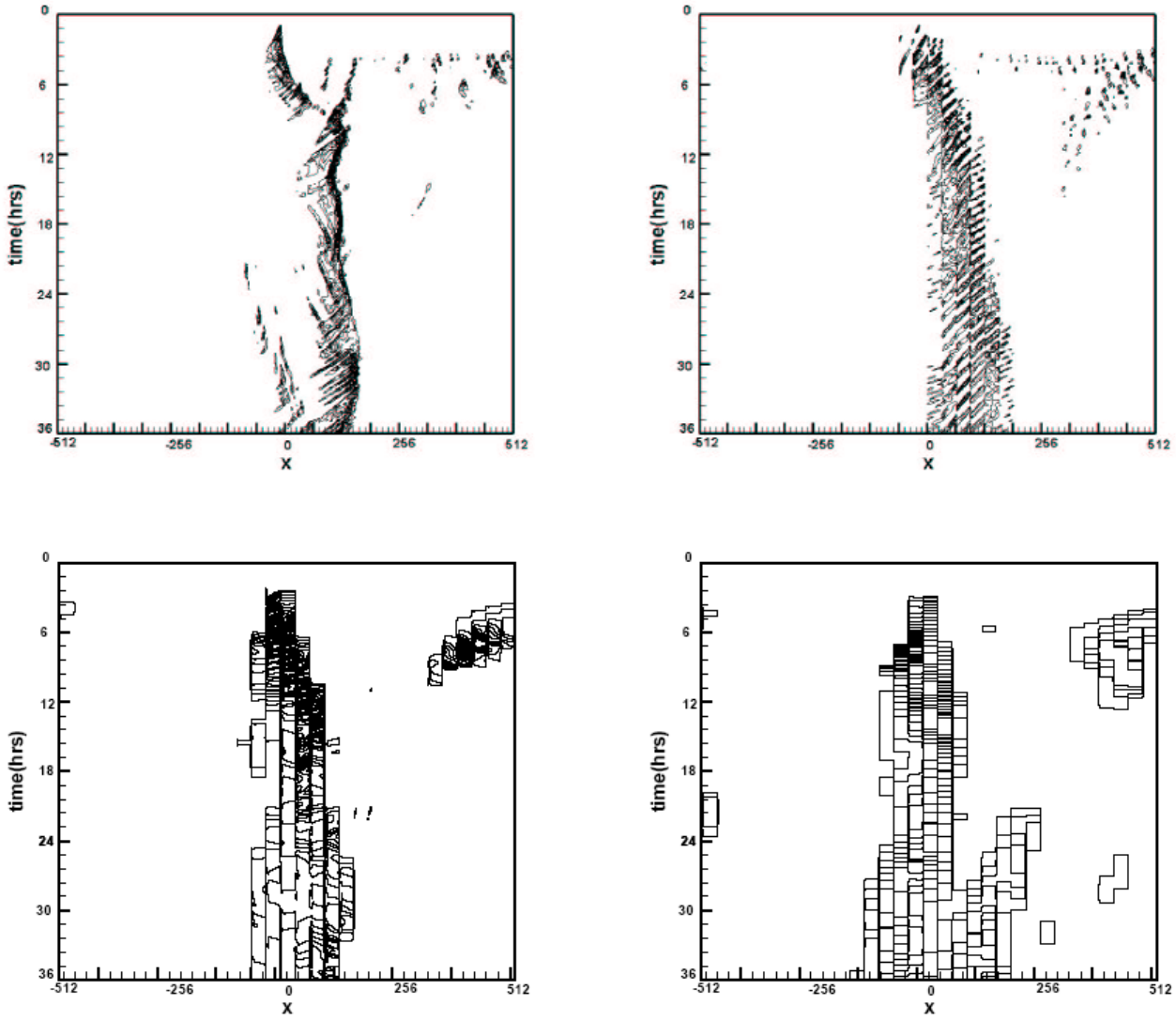

# Large scale features

The time averaged numerical solution of horizontal velocity between 18th and 23rd hours, is denoted by $\langle \bar{u} \rangle$,

Thus the large scale velocity, on mesoscales of order 100 km, is defined as

$$\langle \bar{u} \rangle(x) = \frac{1}{96} \int_{-48}^{48} \langle u \rangle(x+s) ds,$$

and the spatial fluctuation is

$$\langle u' \rangle(x) = \langle u \rangle(x) - \langle \bar{u} \rangle(x).$$

Fig 2. The contours of the large scale horizontal velocity when a=1.
Top left: CRM; Top right: SP; Bottom left: SSTSP3; Bottom right: SSTSP6.

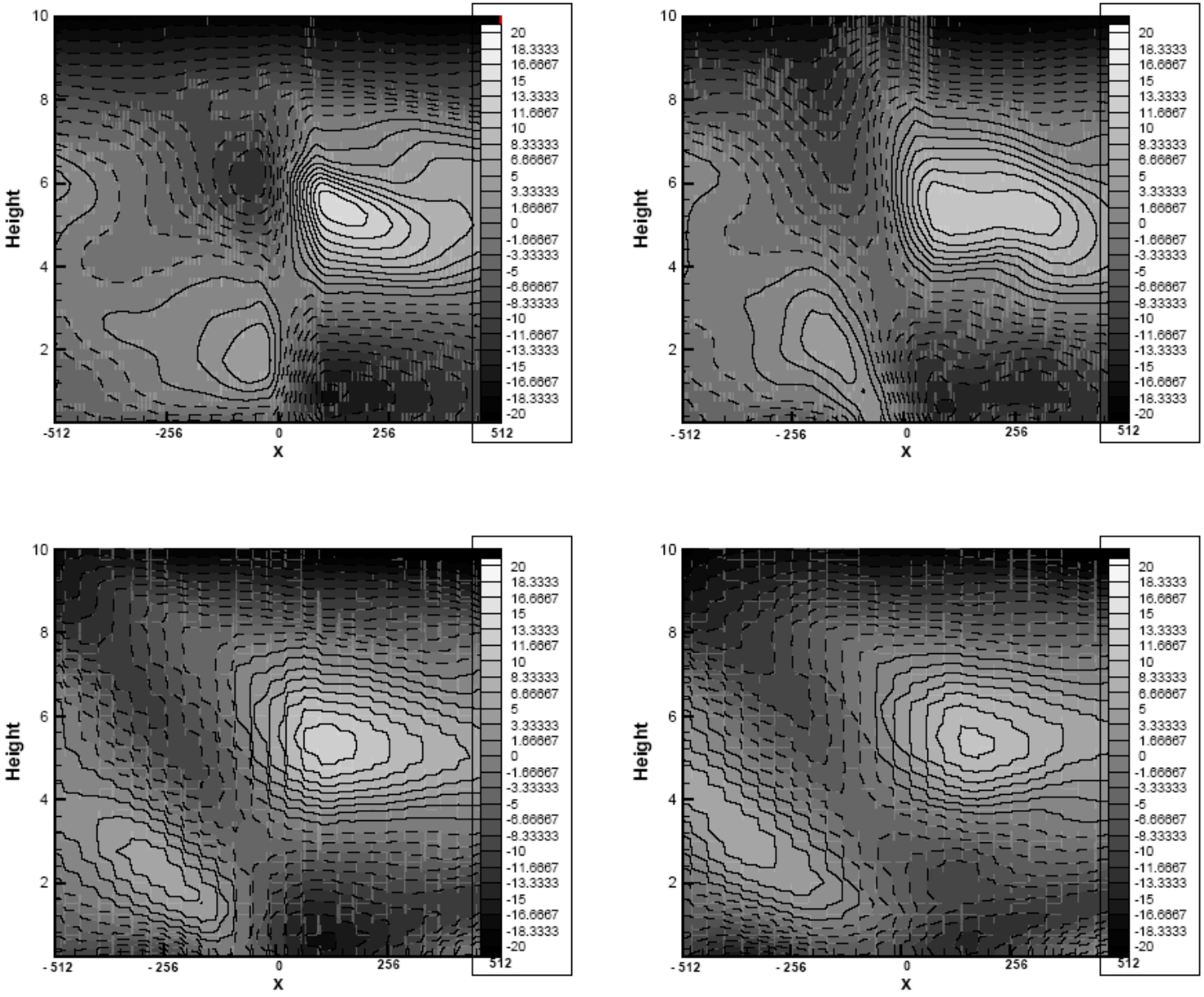

Fig 3. The contours of the large scale specific humidity when a=1.
Top left: CRM; Top right: SP; Bottom left: SSTSP3; Bottom right: SSTSP6.

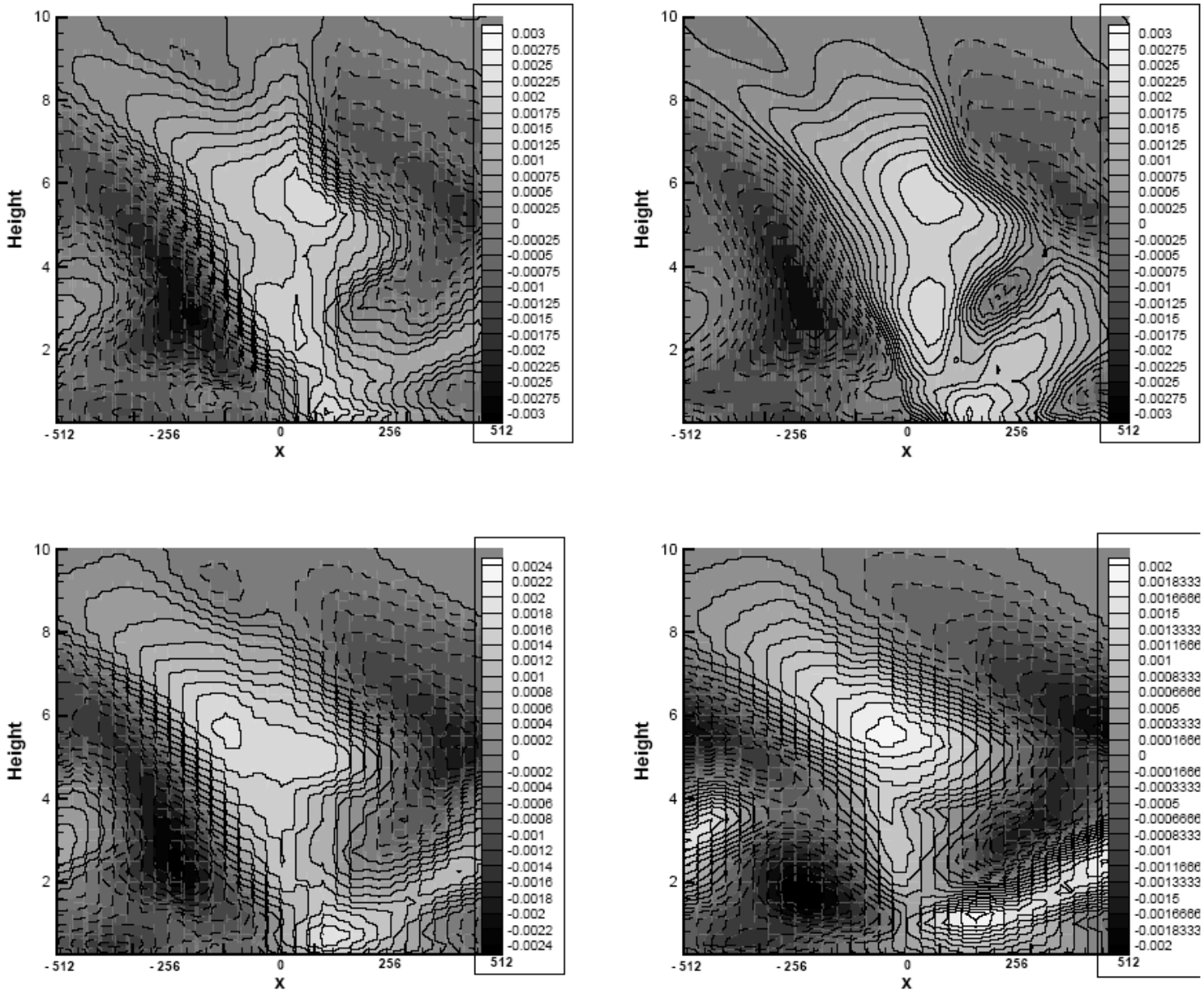

# Test case with a=1

We compute the correlation between these plots.

| | Between SP and SSTSP2 | Between SP and SSTSP3 | Between SP and SSTSP6 |
|---|---|---|---|
| $\langle \bar{q}_v \rangle$ | 0.9417 | 0.8738 | 0.7168 |
| $\langle \bar{\theta} \rangle$ | 0.9104 | 0.7795 | 0.5878 |
| $\langle \bar{u} \rangle$ | 0.9025 | 0.8621 | 0.5876 |
| | Between CRM and SSTSP2 | Between CRM and SSTSP3 | Between CRM and SSTSP6 |
| $\langle \bar{q}_v \rangle$ | 0.8521 | 0.7781 | 0.6571 |
| $\langle \theta \rangle$ | 0.8425 | 0.7325 | 0.5356 |
| $\langle \bar{u} \rangle$ | 0.8735 | 0.8082 | 0.6215 |

These large scale variables are the most important thing to examine as the output in a squall line.

# Test case with a=1

The correlation shows nice structural agreement.

SSTSP3 captures the main large scale effect of the squall line experiment well in a statistically way, and save the computational cost by a factor of roughly 9, compared with the original SP.

Even SSTSP6 has pattern correlation above 0.6 for velocity and humidity.

Fig 4. The contours of the eddy flux divergence - $\overline{(\langle u' \rangle \langle w' \rangle)_z}$ when a=1.
Top left: CRM; Top right: SP; Bottom left: SSTSP3; Bottom right: SSTSP6.

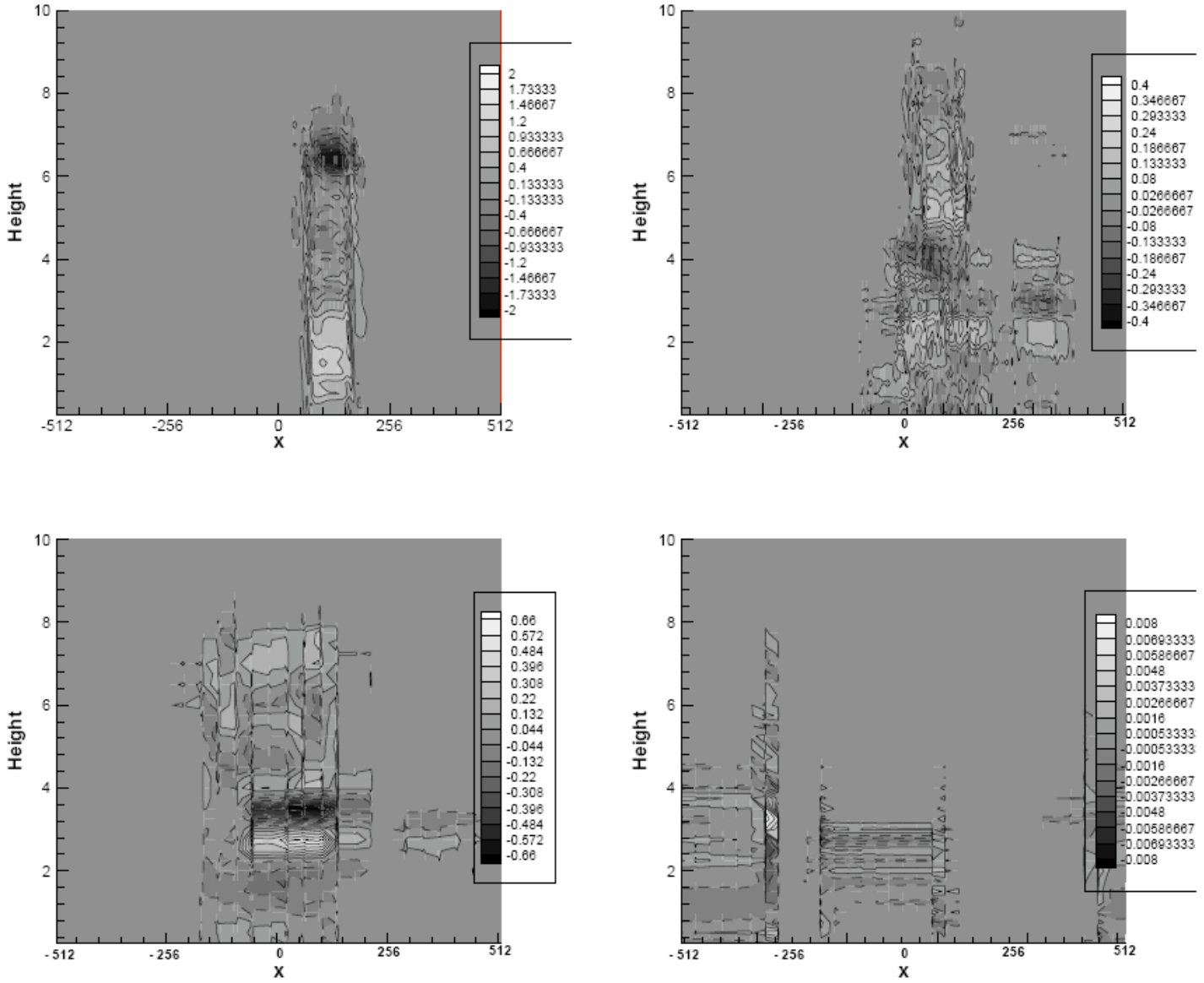

# Test case with a=1

To emphasize that the small scale models play an important role in capturing the squall line:

Run the CRM code with very coarse 32 km resolution, the resolution for the large scale model of the SP test.

No squall line is developed on such coarse meshes. The resolution is too big to capture those cloud scale effects.

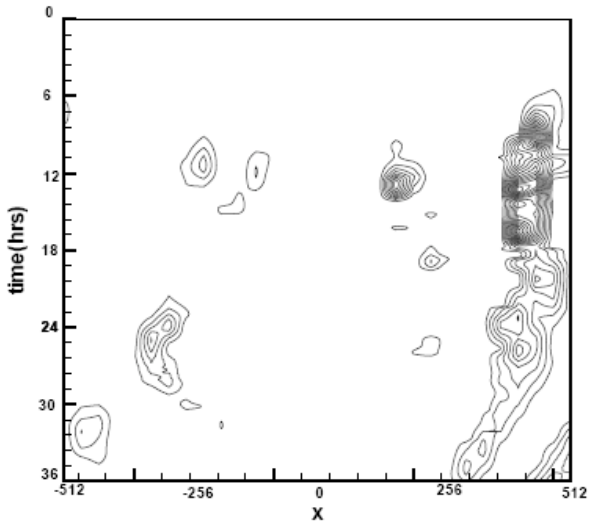


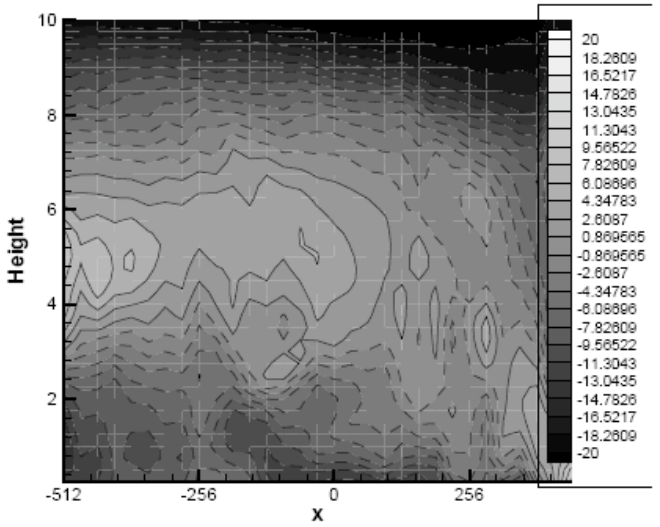


Left: Surface Precipitation; Right: Large scale horizontal velocity.

# Test case with a=0.3

**A weaker shear with a=0.3**

CRM shows that the turbulent travelling wave will decay and not propagate in time.

The SSTSP3 and SSTSP6 both capture this fact.

SSTSP algorithms not only capture the large scale features when a squall line is developed, but also have significant skill in the situation when no quasi-steady squall line is formed.

Fig 5. The contours of the surface precipitation when a=0.3.
Top left: CRM; Top right: SP; Bottom left: SSTSP3; Bottom right: SSTSP6.

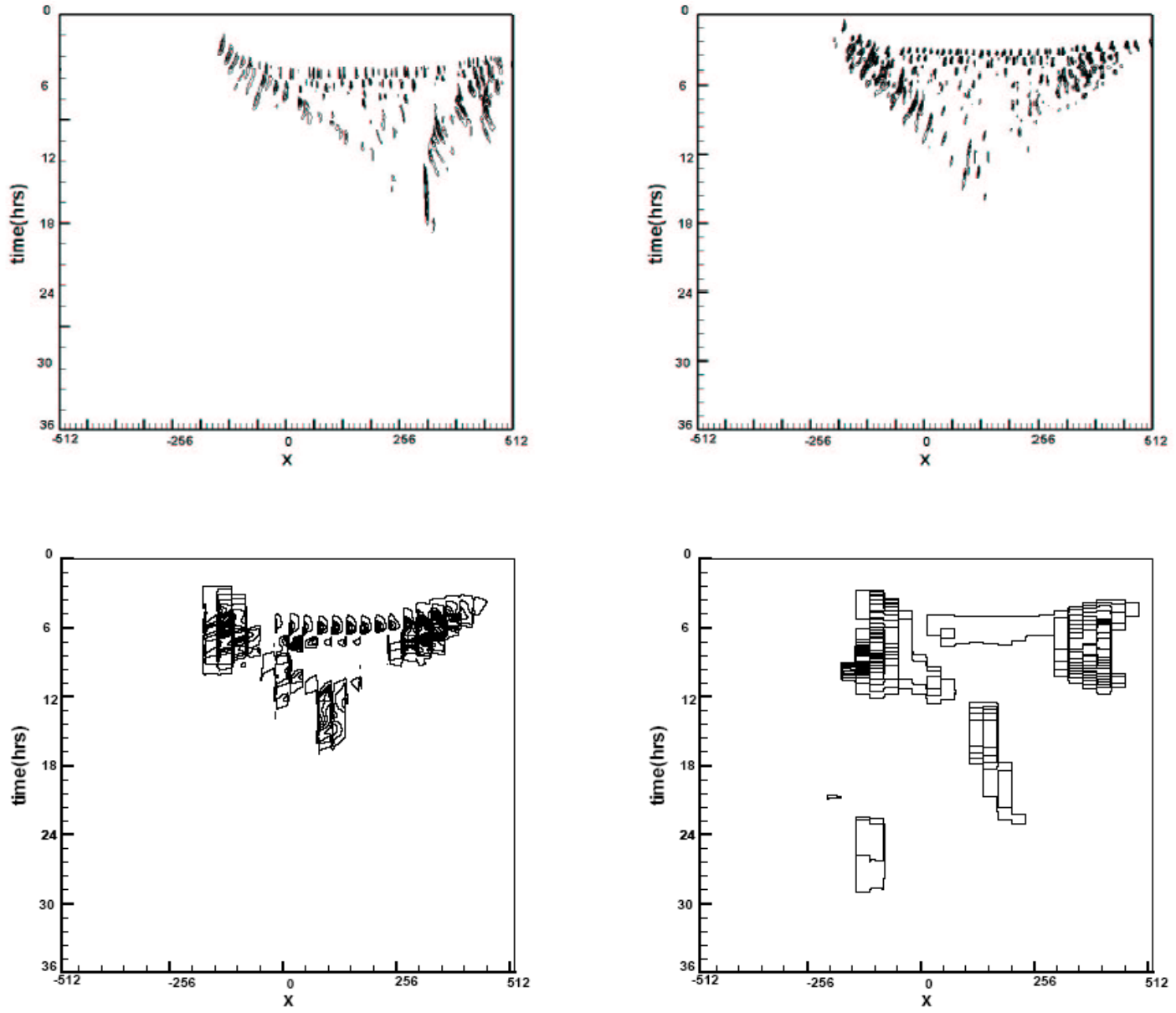

# Test case with a=0.8

For a weaker shear with a=0.8:

correlation between these large scale variables:

| | Between SP and SSTSP2 | Between SP and SSTSP3 | Between SP and SSTSP6 |
|---|---|---|---|
| $\langle \bar{q}_v \rangle$ | 0.9214 | 0.8512 | 0.7064 |
| $\langle \bar{\theta} \rangle$ | 0.8956 | 0.7546 | 0.5779 |
| $\langle \bar{u} \rangle$ | 0.9011 | 0.8451 | 0.5924 |
| | Between CRM and SSTSP2 | Between CRM and SSTSP3 | Between CRM and SSTSP6 |
| $\langle \bar{q}_v \rangle$ | 0.8432 | 0.7623 | 0.6352 |
| $\langle \bar{\theta} \rangle$ | 0.8552 | 0.7243 | 0.5523 |
| $\langle \bar{u} \rangle$ | 0.8834 | 0.8145 | 0.6734 |

Fig 6. The contours of the large scale horizontal velocity when a=0.8.
Top left: CRM; Top right: SP; Bottom left: SSTSP3; Bottom right: SSTSP6.

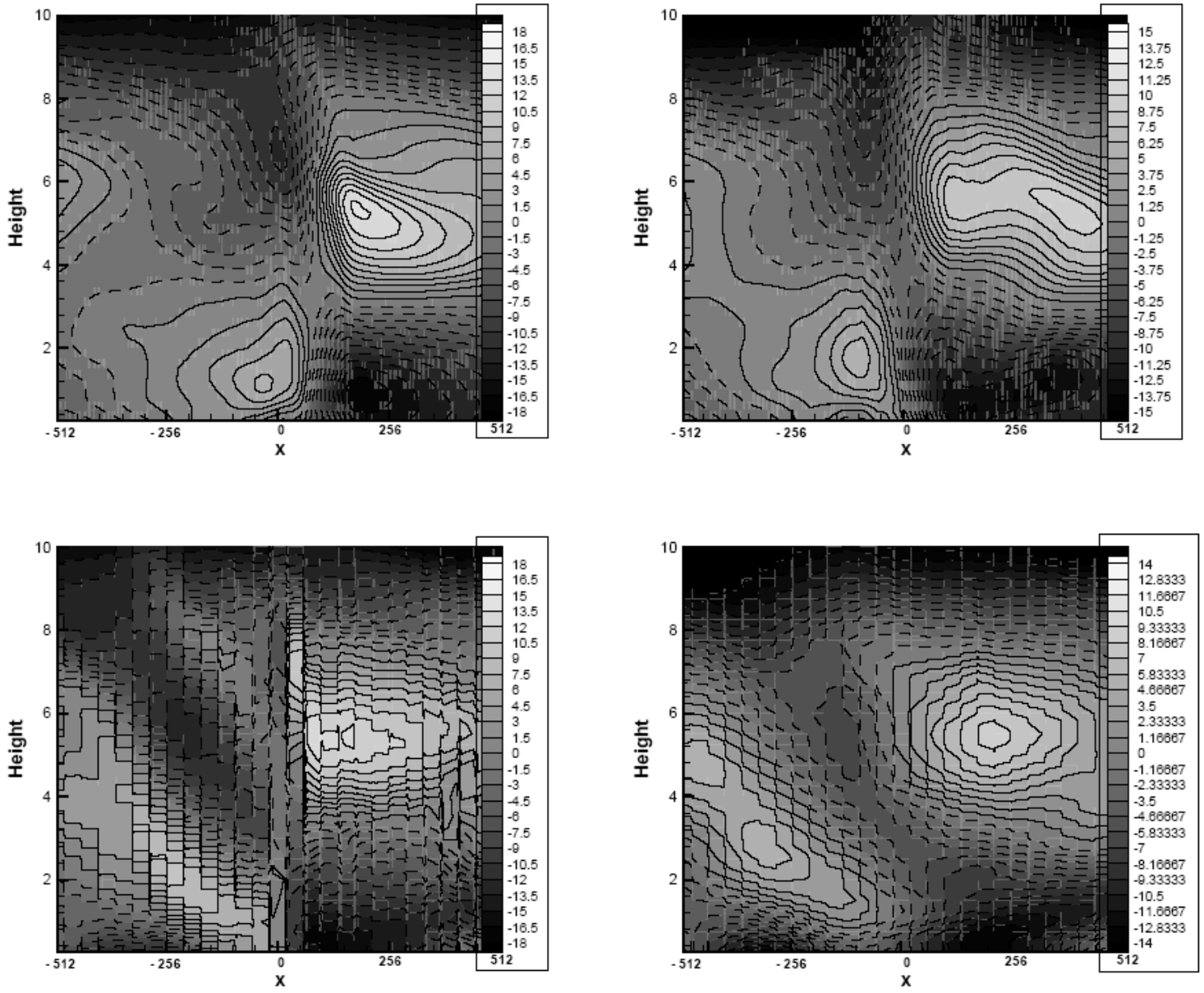

Fig 7. The contours of the large scale specific humidity when a=0.8.
Top left: CRM; Top right: SP; Bottom left: SSTSP3; Bottom right: SSTSP6.

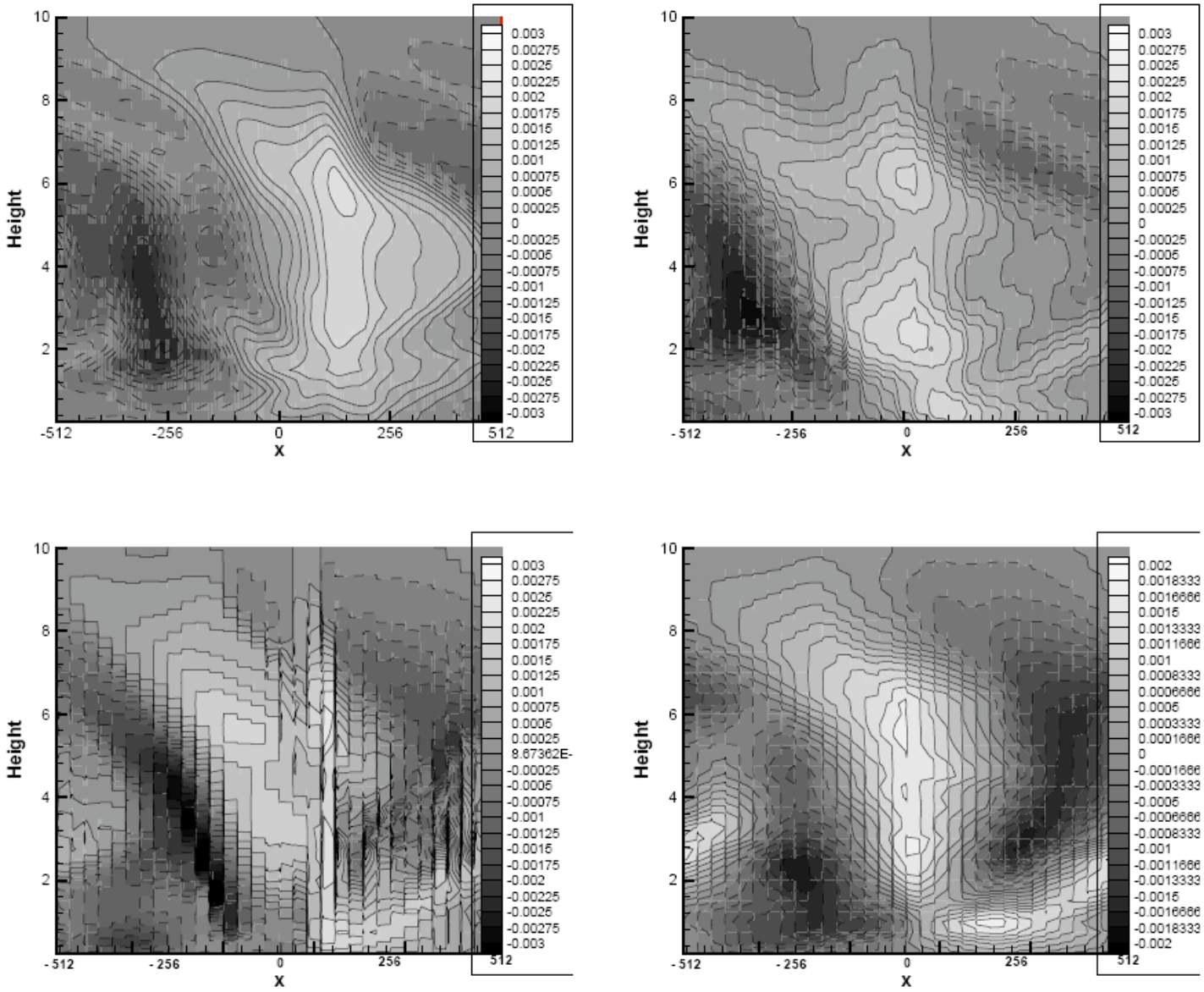

# Test case with a=0.5

For a weaker shear with a=0.5:

correlation between these large scale variables:

| | Between SP and SSTSP2 | Between SP and SSTSP3 | Between SP and SSTSP6 |
|---|---|---|---|
| $\langle \bar{q}_v \rangle$ | 0.8932 | 0.8022 | 0.6573 |
| $\langle \bar{\theta} \rangle$ | 0.8523 | 0.7223 | 0.5321 |
| $\langle \bar{u} \rangle$ | 0.8556 | 0.8023 | 0.6134 |
| | Between CRM and SSTSP2 | Between CRM and SSTSP3 | Between CRM and SSTSP6 |
| $\langle \bar{q}_v \rangle$ | 0.8154 | 0.7235 | 0.6154 |
| $\langle \theta \rangle$ | 0.8242 | 0.7054 | 0.5254 |
| $\langle \bar{u} \rangle$ | 0.8573 | 0.7654 | 0.6248 |

Fig 8. The contours of the large scale horizontal velocity when a=0.5.
Top left: CRM; Top right: SP; Bottom left: SSTSP3; Bottom right: SSTSP6.

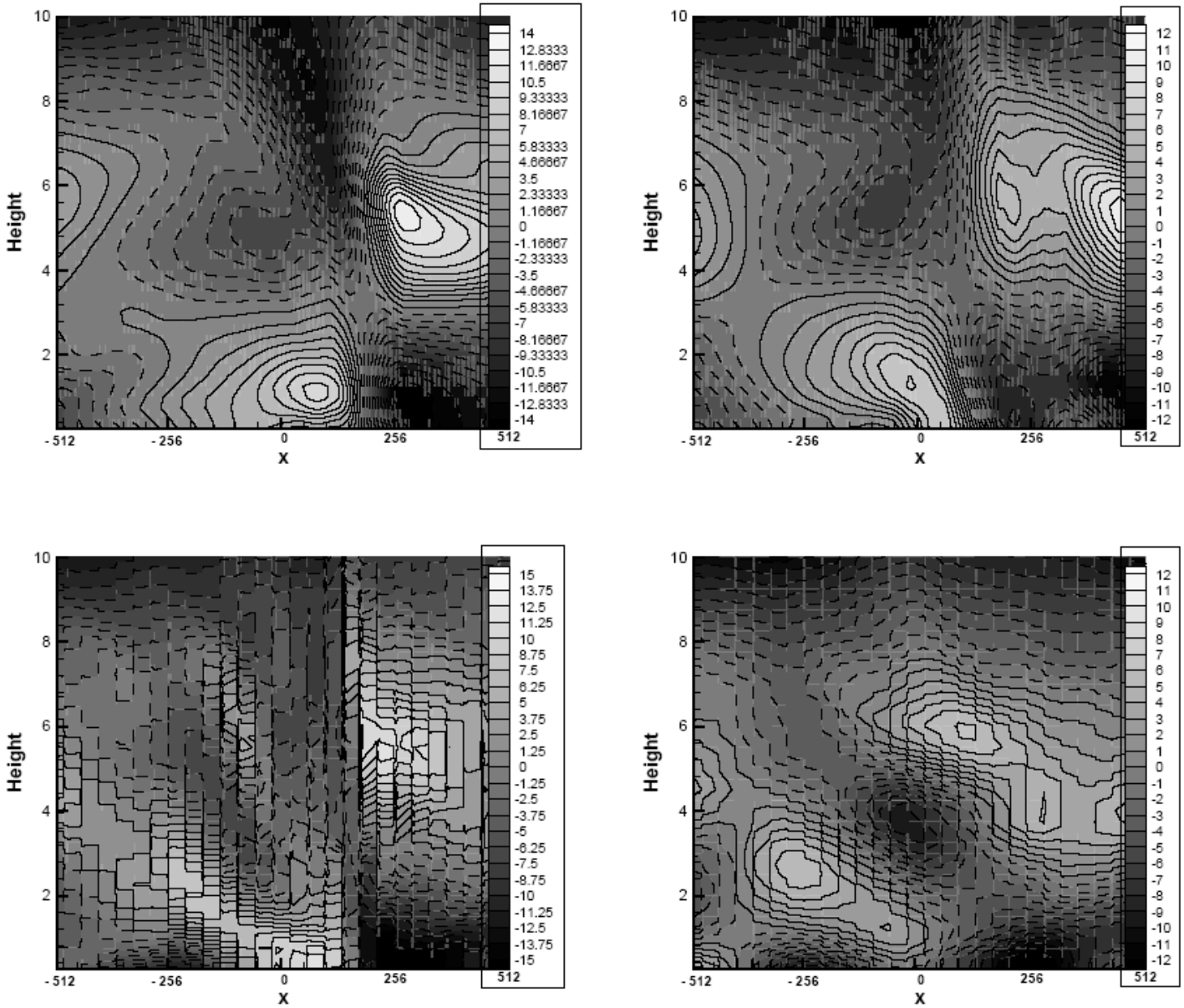

Fig 9. The contours of the large scale specific humidity when a=0.5.
Top left: CRM; Top right: SP; Bottom left: SSTSP3; Bottom right: SSTSP6.

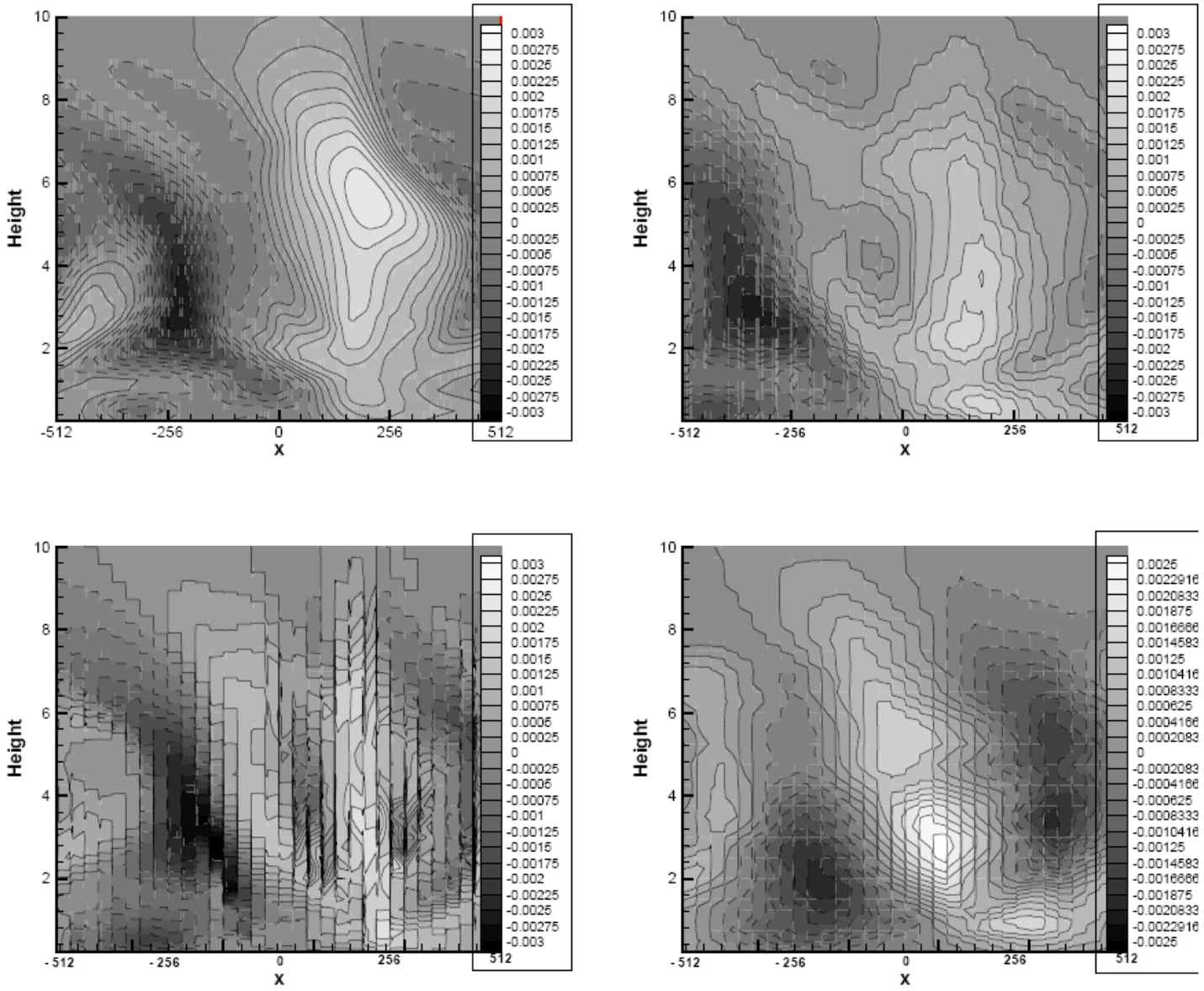

# A propagating squall line

We modify this experiment to obtain a propagating squall line.

A different background shear U(z) (obtained from reality) is used.

We show the jet max and mean propagation speed of the squall line:

| | CRM | SP | SSTSP2 | SSTSP3 | SSTSP6 |
|---|---|---|---|---|---|
| Jet max(km) | 14.1 | 14.1 | 14.1 | 14.1 | 14.1 |
| Squall line speed (m/s) | 11.5 | 10.5 | 10 | 10 | 10 |

Both the SSTSP3 and SSTSP6 cases reproduce the squall line speed in the CRM within 10%

Fig 10. The contours of the surface precipitation for a propagating squall line. Top left: CRM; Top right: SP; Bottom left: SSTSP3; Bottom right: SSTSP6.

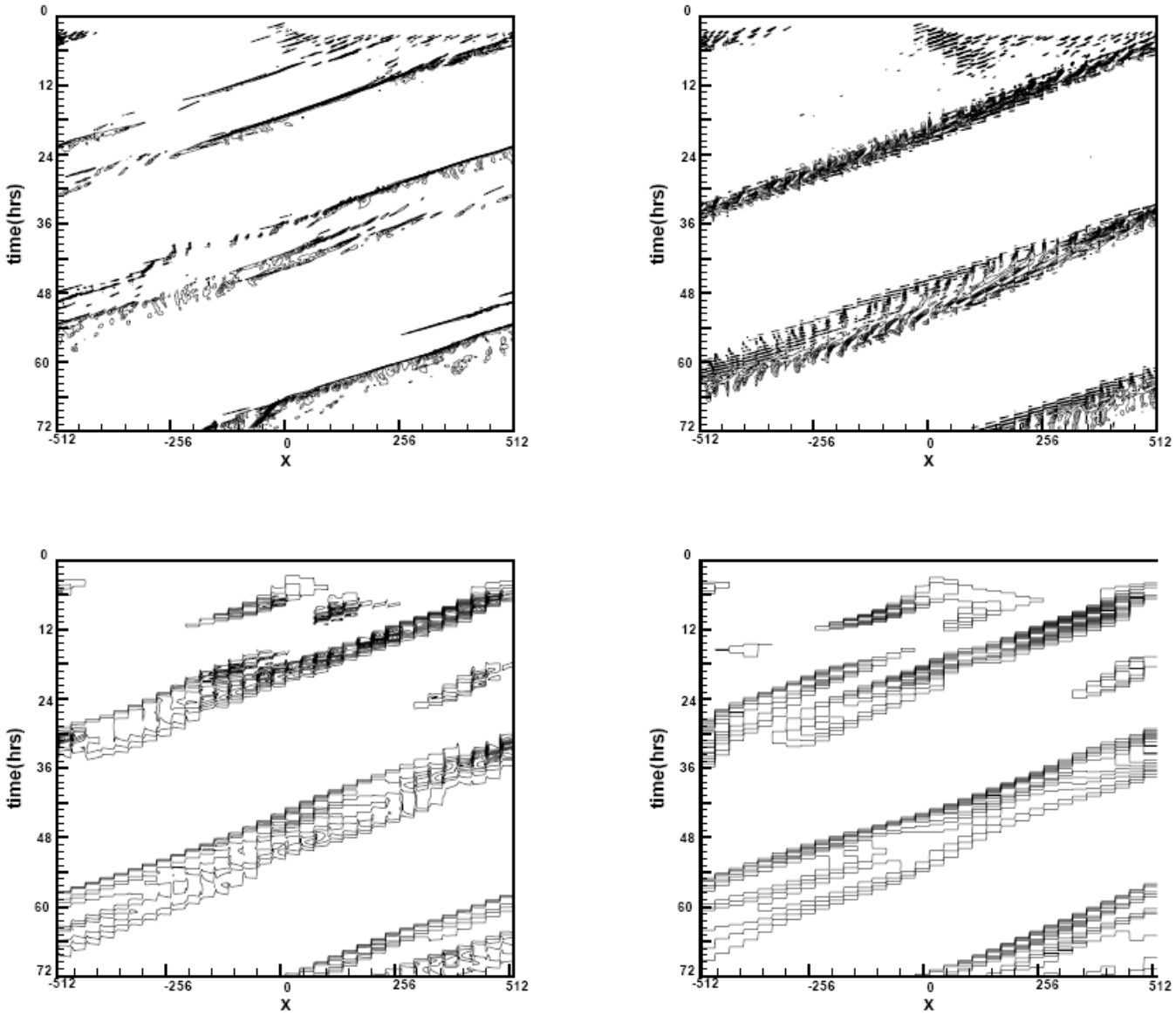

# Summary

We show:

- SSTSP3 results in a gain of roughly a factor of 10 in efficiency, and captures large scale variables, such as velocity and specific humidity, in a reasonably statistically accurate way (with correlation above 0.75).

- SSTSP6 algorithm, with 1/36 computational cost, has pattern correlation above 0.6 for large scale velocity and humidity.

- The structure of eddy momentum flux divergence, positive region below and negative region above, is captured qualitatively by SP and SSTSP3. SSTSP6 fails in capturing this fact.

# Thank You